INFECTION AND IMMUNITY, July 2008, p. 3312–3320 Vol. 76, No. 7
0019-9567/08/$08.00+0 doi:10.1128/IAI.01475-07

Common Strategies To Prevent and Modulate Experimental Cerebral Malaria in Mouse Strains with Different Susceptibilities▽†

Louise M. Randall,[1,2] Fiona H. Amante,[1] Karli A. McSweeney,[1] Yonghong Zhou,[1] Amanda C. Stanley,[1] Ashraful Haque,[1] Malcolm K. Jones,[1] Geoff R. Hill,[1] Glen M. Boyle,[1] and Christian R. Engwerda[1]*

Queensland Institute of Medical Research, 300 Herston Road, Herston, Queensland 4006, Australia,[1] and School of Population Health, Public Health Building, University of Queensland, Herston Road, Herston, Queensland 4006, Australia[2]

Received 4 November 2007/Returned for modification 13 December 2007/Accepted 3 May 2008

Cerebral malaria (CM) is a severe complication of *Plasmodium falciparum* infection, predominantly experienced by children and nonimmune adults, which results in significant mortality and long-term sequelae. Previous studies have reported distinct susceptibility gene loci in CBA/CaH (CBA) and C57BL/6 (B6) mice with experimental CM (ECM) caused by infection with *Plasmodium berghei* ANKA. Here we present an analysis of genome-wide expression profiles in brain tissue taken from B6 and CBA mice with ECM and report significant heterogeneity between the two mouse strains. Upon comparison of the leukocyte composition of ECM brain tissue, microglia were expanded in B6 mice but not CBA mice. Furthermore, circulating levels of gamma interferon, interleukin-10, and interleukin-6 were significantly higher in the serum of B6 mice than in that of CBA mice with ECM. Two therapeutic strategies were applied to B6 and CBA mice, i.e., (i) depletion of regulatory T (Treg) cells prior to infection and (ii) depletion of $CD8^+$ T cells after the establishment of ECM. Despite the described differences between susceptible mouse strains, depletion of Treg cells before infection attenuated ECM in both B6 and CBA mice. In addition, the depletion of $CD8^+$ T cells when ECM symptoms are apparent leads to abrogation of ECM in B6 mice and a lack of progression of ECM in CBA mice. These results may have important implications for the development of effective treatments for human CM.

Cerebral malaria (CM) is a severe neurological complication that arises predominantly in children and nonimmune adults infected with *Plasmodium falciparum* parasites. In sub-Saharan Africa, it has been estimated that CM affects around 500,000 people each year, resulting in case fatality rates of 17.5 to 19.2% and long-term neurological sequelae in many CM survivors (9, 30, 31, 45). CM has been associated with the sequestration of parasitized red blood cells (pRBC) in the brain microvasculature (1, 35), with the accumulation of mononuclear cells in brain tissue (37), and with the increased expression of proinflammatory cytokines (10) such as tumor necrosis factor (TNF) both in the brain and systemically (7, 19, 23, 25). A large proportion of deaths occur in hospitals before antiparasitic treatment can take effect (15), highlighting the importance of understanding the pathogenesis of this disease and of implementing new, rapidly acting interventions in combination with antiparasitic treatment (50).

Experimental CM (ECM) caused by infection of C57BL/6 (B6) or CBA/CaH (CBA) mice with *Plasmodium berghei* ANKA displays many features of human CM and has been useful in identifying host factors involved in CM pathogenesis. The host immune response to parasites plays a significant role in ECM. Conventional dendritic cells (14), $CD4^+$ and $CD8^+$ T cells (5, 6, 22, 49), natural regulatory T (Treg) cells (3, 48), NK T cells (21, 41), NK cells (20), and platelets (26, 46, 47) have been implicated in ECM and appear to play a negative role in disease outcome. In addition, several pro- and anti-inflammatory cytokines have been shown to influence the outcome of ECM pathogenesis. These include gamma interferon (IFN-γ; 2, 19, 49), TNF (18), lymphotoxin alpha (LTα; 16), and interleukin-10 (IL-10) (24). All of these cytokines, except IL-10, play negative roles in disease outcome. Interestingly, susceptibility/resistance loci have been mapped to different chromosomes within the genome of CBA and B6 mice (4, 32, 34), indicating that factors critical to ECM development may be different between the two strains of mice (34). This is consistent with human CM, which is considered to be a syndrome with significant heterogeneity in disease development and manifestation between affected individuals (11, 27).

In this study, we investigated changes in gene expression in brain tissue following the development of severe ECM symptoms in B6 and CBA mice. We also examined immune responses in these different mouse strains throughout *P. berghei* ANKA infection. We found significant heterogeneity in brain gene expression profiles between B6 and CBA mice with ECM and many differences in the immune responses of these mouse strains to *P. berghei* ANKA infection. However, modulating the function of Treg cells could prevent ECM and depletion of $CD8^+$ cells could treat ECM in both mouse strains. These data indicate that common strategies might be used to prevent CM across a broad population base.

* Corresponding author. Mailing address: Queensland Institute of Medical Research, 300 Herston Road, Herston, QLD 4006, Australia. Phone: 61 7 3362 0428. Fax: 61 7 3362 0104. E-mail: Christian.Engwerda@qimr.edu.au.

† Supplemental material for this article may be found at http://iai.asm.org/.

▽ Published ahead of print on 12 May 2008.

MATERIALS AND METHODS

Mice and infections. Female B6 and CBA mice (5 to 6 weeks of age) were from the Animal Resources Centre (Canning Vale, Western Australia). Mice were infected with *P. berghei* ANKA pRBC, and blood parasitemia, anemia, and ECM symptoms were monitored by using a clinical score system as previously described (3, 14). Age-matched naive B6 and CBA mice were included as controls. All procedures were approved by the Queensland Institute of Medical Research Animal Ethics Committee.

Sample preparation and RNA extraction. Mice were sacrificed by CO_2 asphyxiation, and blood was obtained by cardiac puncture for serum cytokine analyses. Mice were then perfused with 20 ml ice-cold phosphate-buffered saline via the heart in order to remove blood and other nonadherent cells from the brain microvasculature. Brains were isolated, halved, and preserved in either RNA*later* (Qiagen, Doncaster, Australia) or Tissue-Tek O.C.T. Compound (Sakura, Torrance, CA). Total RNA was extracted from brain tissue as previously described (3), and RNA quality was assessed with RNA 6000 Nano Assay Kits on a Bioanalyzer 2100 (Agilent Technologies, Forest Hill, Australia). Samples included in this study had 260:280-nm absorbance readings between 1.8 and 2.0. Equal quantities of six samples of naïve and *P. berghei* ANKA-infected brain tissue from B6 and CBA mice were pooled for microarray analysis.

Expression profiling with microarrays. Pooled RNA samples were converted to cDNA and antisense cRNA, labeled, and hybridized to GeneChip Mouse Genome 430 2.0 arrays (Affymetrix, Surrey Hills, Australia) by the Australian Genome Research Facility (Parkville, Australia) according to Affymetrix protocols. Each array analyzed the expression of more than 39,000 transcripts and variants representing the entire mouse transcribed genome. Arrays were scanned with the GeneChip Scanner 3000 (Affymetrix) and GeneChip Operating Software v1.1.1 (Affymetrix). Normalization and initial analyses were carried out in GeneSpring v7 (Agilent Technologies). Values below 0.01 were set to 0.01. Each measurement was divided by the 50th percentile of all measurements in that sample. The data were filtered for genes flagged as present which had an expression level of at least 50 Affymetrix units, a measurement of signal intensity generated directly from Affymetrix chips. The samples analyzed had similar numbers of transcripts and variants tagged as present on the arrays (naïve CBA, 25,801; CBA ECM, 25,833; naïve B6, 26,407; B6 ECM, 26,437). Overall, when focusing on naïve brain tissue, 24,033 probes were tagged as present in both naïve CBA and B6 brain tissue while only 1,800 and 2,404 probes were tagged as uniquely present in naïve B6 or CBA brain tissue, respectively. To determine differences in gene expression profiles, the ECM samples were normalized to the naive sample such that each measurement for each gene in the ECM samples was divided by the median of that gene's measurements in the corresponding naïve sample. All of the pooled ECM samples (B6 and CBA separately) were then independently considered to be duplicate samples of each other for statistical analyses. Likewise, the naïve samples (B6 and CBA separately) were also treated as duplicates. This consideration generated two ratio values for each treatment group (naïve and ECM). A *t* test was then used to analyze whether the expression of each probe set in the ECM sample was significantly different from the naïve brain sample for each CBA or B6 mouse. Transcripts were deemed to be differentially expressed when the *P* value was equal to or less than 0.05.

Once normalized, 98 transcripts were found to be expressed significantly more in naïve CBA brain tissue than in naïve B6 brain tissue. Importantly, the increased level of these transcripts in naïve tissue did not result in higher expression in CBA ECM brain tissue. Likewise, 181 transcripts were found to have a higher resting expression levels in naïve B6 brain tissue than in naïve CBA brain tissue. Of these, only six genes were also found to be significantly upregulated in B6 ECM brain tissue. Therefore, differences in brain gene expression profiles observed between the two strains are likely to reflect differences in cellular recruitment, responses to the presence of parasites, and signaling pathways initiated in the brain during ECM rather than simply to reflect variations in experimental conditions.

Real-time RT-PCR. Individual RNA samples were reverse transcribed into cDNA with the cDNA Archive Kit (Applied Biosystems, Scoresby, Australia). Real-time reverse transcription (RT)-PCR analyses were performed on a Corbett Rotorgene 3000 (Corbett Life Sciences, Sydney, Australia). Platinum SYBR green master mix (Invitrogen) was used when measuring TNF (5′GGTACAAC CCATCGGCTGGCA [forward] and 5′GATTCAACCTTGCGCTCATCTT AGGC [reverse]), LTα (5′CTGCTCACCTTGTTGGGTACCC [forward] and 5′GACAAAGTAGAGGCCACTGGTG [reverse]), LTβ (5′CTCAGAGATCC AATGCTTCC [forward] and 5′CCAAGCGCCTATGAGGTG [reverse]), TNFR1 (5′GCCACAAAGGAACCTACTTGG [forward] and 5′CACTCAGGT AGCGTTGGAACTGG [reverse]), and TNFR2 (5′GAAAACCCATTCTGGC AGCTGTCG [forward] and 5′CAGGATGCTACAGATGCGGTGG [reverse]) mRNA levels. All measurements were normalized against the expression of the hypoxanthine phosphoribosyltransferase housekeeping gene (5′GTTGGATAC AGGCCAGACTTTGTTG [forward] and 5′GATTCAACCTTGCGCTCATCT TAGGC [reverse]).

Anti-CD8 monoclonal antibody (MAb) and anti-CD25 MAb treatment. B6 and CBA mice were depleted of Treg cells by the administration of a single intraperitoneal (i.p.) injection of 0.5 mg anti-CD25 MAb (PC61; rat immunoglobulin G1 [IgG1]; American Type Culture Collection, Manassas, VA) either 1 or 14 days prior to *P. berghei* ANKA infection. Mice were depleted of $CD8^+$ T cells when ECM symptoms were apparent and all clinical scores in the group were above 2. Animals received a single i.p. injection of 0.5 mg of anti-CD8α MAb (YTS169.1; rat IgG2a; European Collection of Cell Cultures, Porton Down, United Kingdom). The efficiency of Treg cell and $CD8^+$ T-cell depletion was tested by flow cytometry in each experiment performed.

Assessment of cell types in brain tissue. Brain tissue was collected into collagenase solution (1 mg/ml type IV collagenase [Worthington, Lakewood, NJ] and 0.5 mg/ml DNase I [Worthington] in RPMI medium) prior to the isolation of brain mononuclear cells for fluorescence-activated cell sorter (FACS) analysis, as previously described (3). Cells were stained for CD4 (clone GK1.5), CD8 (clone 53-6.7), TCRβ (clone H57-597), NK1.1 (clone PK136), B220 (clone RA3-6B2), CD19 (clone 6D5), CD11b (clone M1/70), Ly6C (clone AL-21), Ly6G (clone 1A8), CD11c (clone N418), or CD45.2 (clone 104) expression with anti-mouse MAbs purchased from BD Bioscience or Biolegend, and cell populations were defined as previously described (3).

Measurement of serum cytokine levels. Serum was collected prior to the commencement of experiments and on day 5 p.i. or at ECM onset via the tail vein. Blood samples were allowed to clot overnight at 4°C, and sera were collected following centrifugation. Cytokines in individual serum samples were quantified with the Cytometric Bead Array Inflammatory kit (BD Bioscience) on a FACScan cytometer equipped with CellQuest Pro and CBA software (BD Bioscience).

In vivo bioluminescence imaging. In some experiments, mice were infected with *P. berghei* ANKA transgenic for a luciferase gene. The location of parasites in vivo, as well as the bioluminescence generated, was determined with an I-CCD photon-counting video camera and imaging system (IVIS 100; Xenogen, Alameda, CA) as previously reported (3).

Statistics. Differences in the survival of treatment groups were analyzed by the Kaplan-Meier log rank test with GraphPad Prism version 4.03 for Windows (GraphPad Software, San Diego, CA). Differences in blood parasitemia, cytokine levels, and cell numbers in brain tissue between treatment groups and mouse strains were determined by two-way analysis of variance, followed by a Bonferroni post-hoc test with GraphPad Prism. For all statistical tests, $P < 0.05$ was considered significant.

Nucleotide sequence accession number. All of the nucleotide sequence data obtained in this study have been submitted to the Gene Expression Omnibus (GEO) and accepted and can be accessed by using accession number GSE6019 (http://www.ncbi.nih.gov/geo/).

RESULTS

Brain gene expression profiles are heterogeneous in CBA and B6 mice with ECM. B6 and CBA mice developed neurological symptoms within a 24-h window following *P. berghei* ANKA infection with no difference in blood parasitemia on the day of sacrifice (day 6 p.i.; Fig. 1A and B). Brains were removed from these animals to investigate gene expression profiles. Brains were also collected from naïve B6 and CBA mice to enable the measurement of constitutive gene expression levels. Following hybridization to Affymetrix GeneChip Mouse Genome 430 2.0 arrays and the performance of statistical analysis as described in Materials and Methods, we found that 221 genes were commonly upregulated during ECM in the brains of both mouse strains (see Table S1 in the supplemental material). Notably, 324 and 498 genes were solely upregulated in B6 (see Table S2 in the supplemental material) and CBA (see Table S3 in the supplemental material) brains with ECM, respectively (Fig. 1C). We also found that 11 genes were commonly downregulated during ECM in both mouse strains,

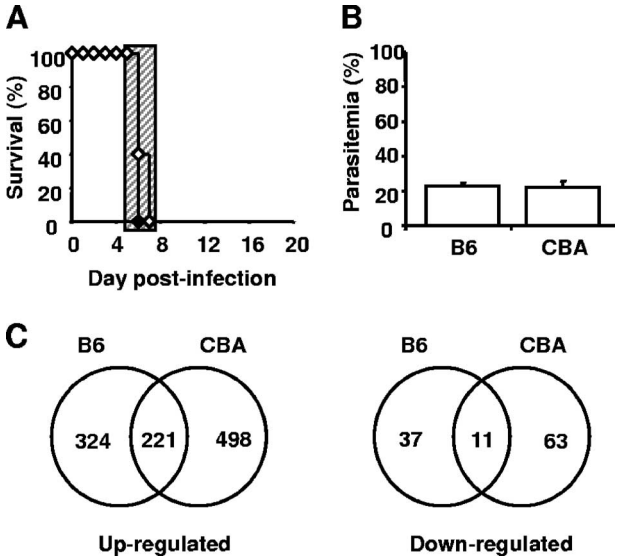

FIG. 1. *P. berghei* ANKA-infected B6 and CBA mice show heterogeneous brain gene expression during ECM. (A) B6 (closed diamonds) or CBA (open diamonds) mice were infected with 10^5 *P. berghei* ANKA pRBC intravenously. Mice were sacrificed upon the development of severe ECM symptoms ($n = 6$ mice per group). The hatched area indicates the time when mice displayed ECM symptoms. (B) Parasitemia was also monitored (mean ± standard error of the mean, $n = 6$ mice per group). (C) RNA was extracted from perfused brain tissue from both *P. berghei* ANKA-infected and naïve CBA and B6 mice and hybridized to Affymetrix GeneChip Mouse Genome 430 2.0 arrays. Total-brain gene expression profiles were compared between CBA and B6 mice based on significant upregulation or downregulation of genes during ECM, following normalization and statistical testing.

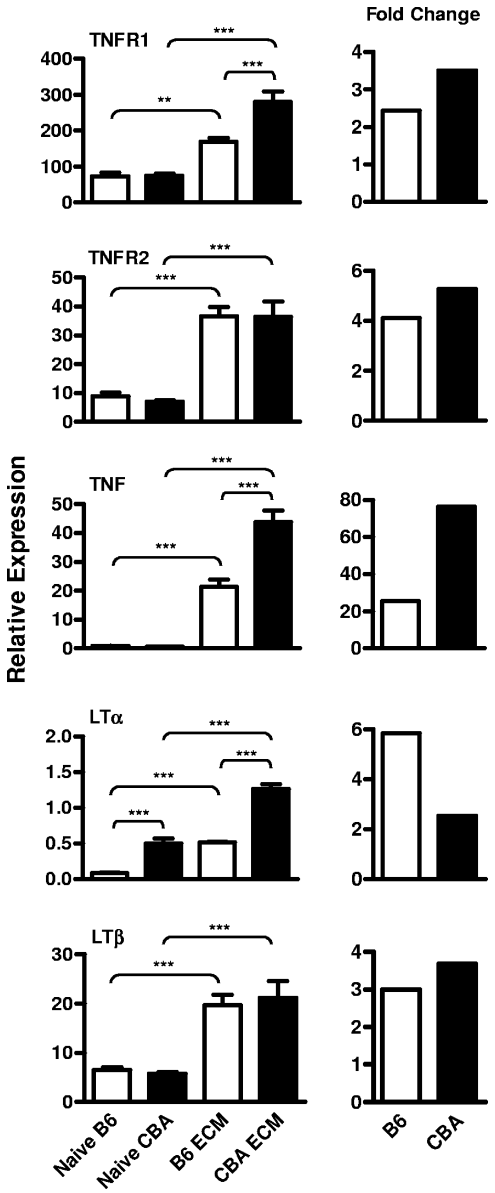

FIG. 2. Differential expression of mRNAs encoding TNF, LTα, and their receptors in ECM brain tissue from *P. berghei* ANKA-infected CBA and B6 mice. TNF, LTα, LTβ, TNFR1, and TNFR2 mRNA levels were measured in brain tissue taken from naïve and *P. berghei* ANKA-infected B6 and CBA mice during ECM, relative to the expression of 1,000 hypoxanthine phosphoribosyltransferase mRNA molecules (mean ± standard error of the mean; $n = 6$ mice per group; left panel). The relative change in the expression of each cytokine or receptor in ECM brain tissue, relative to naïve brain tissue, was also calculated (right panel). The data presented are from one representative experiment of two performed. Statistically significant differences of $P < 0.01$ (**) and $P < 0.001$ (***) are shown.

while 37 genes were solely downregulated in B6 mice and 63 genes were solely downregulated in CBA mice (Fig. 1C). A number of the genes identified in our study have yet to be defined functionally (see accession number GSE6019 at http://www.ncbi.nih.gov/geo/). Importantly, a number of genes previously reported to play key roles in ECM pathogenesis were identified as being significantly upregulated in both mouse strains (see Table S1 in the supplemental material). These include those for heme oxygenase 1 (*hmox1*) (36) and CXCL10 (γIP-10) (20, 29), as well as granzyme A and granzyme B, products of cytolytic $CD8^+$ T cells (5, 38, 49). However, gene expression profiling was performed only once in this study with pooled samples. Therefore, the data were primarily used to provide a general contrast of response to infection between the two mouse strains, as well as a tool for the generation of preliminary hypotheses. Thus, these data indicate extensive heterogeneity in gene expression profiles between B6 and CBA mice and also suggest that CBA mice have greater overall immunological activity in the brain during ECM than B6 mice.

CBA and B6 mice with ECM have differential expression of TNF family members in brain tissue. TNF (18) and LTα (16) have been implicated in the pathogenesis of CM. However, our microarray analysis revealed few changes in TNF family members, although TNFR1 was significantly upregulated in both CBA and B6 mice with ECM (see Table S1 in the supplemental material). Previous microarray studies have reported difficulty in identifying changes in cytokine expression levels (44). For this reason and the potential importance of TNF and LTα in CM pathogenesis, we investigated the expression of these cytokines and their receptors in individual naïve and ECM brains taken from CBA and B6 mice by real-time RT-PCR (Fig. 2). TNFR1 mRNA levels were significantly upregulated during ECM in CBA ($P < 0.001$) and B6 ($P < 0.01$) brain tissue compared with the naïve control brain tissue, validating the microarray results. TNF mRNA levels were significantly

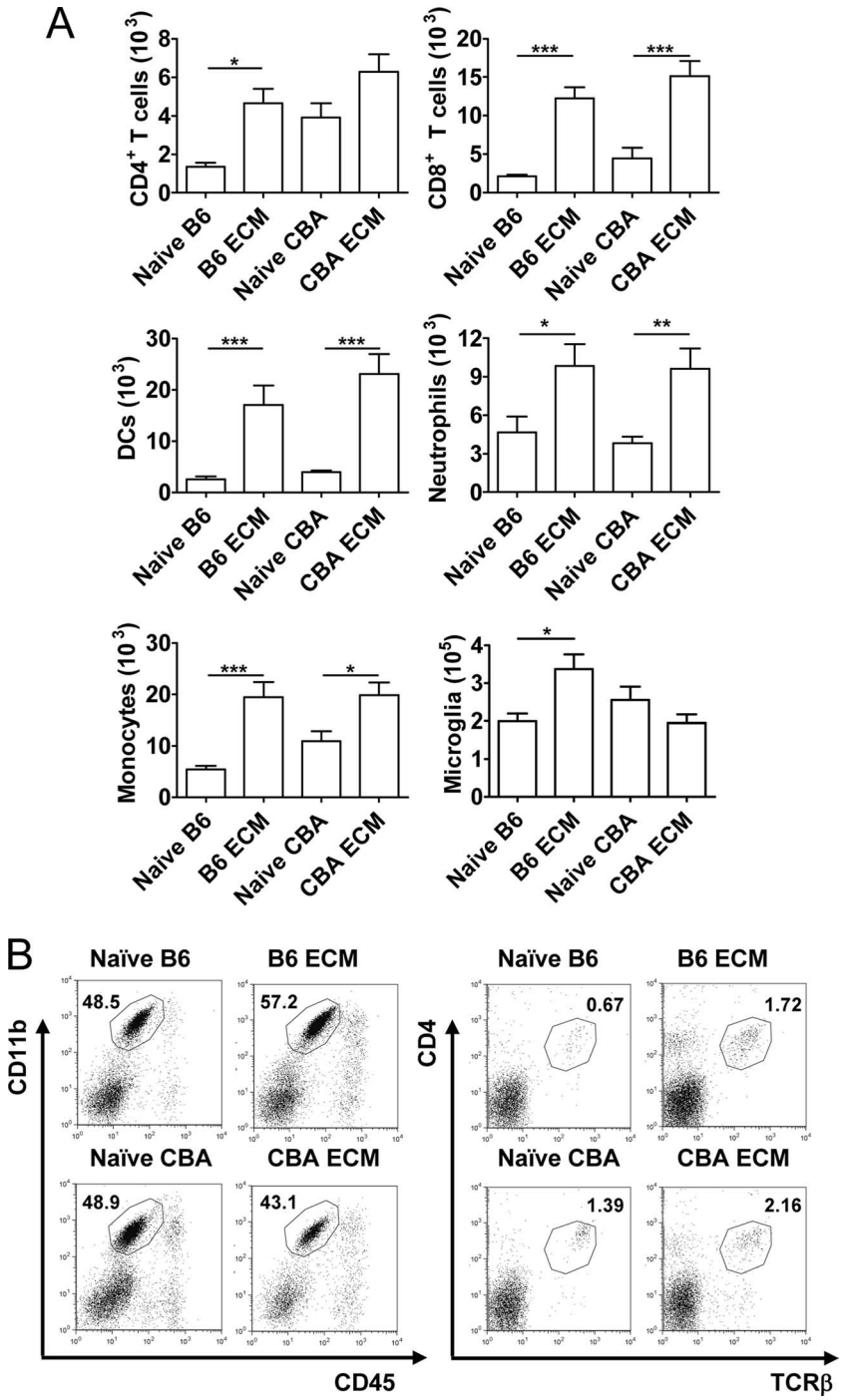

FIG. 3. *P. berghei* ANKA-infected B6 mice show expansion of microglia during ECM. Mononuclear cells were prepared from brain tissue obtained during ECM and analyzed by FACS. The total numbers of $CD4^+$ T cells, $CD8^+$ T cells, DCs, neutrophils, monocytes/macrophages, and microglia were measured in naïve and infected CBA and B6 mouse brain tissue (mean ± standard error of the mean; $n = 5$ mice per group), as indicated (A). Representative FACS profiles of brain $CD4^+$ T cells ($CD4^+$, $TCR\beta^+$) and microglia ($CD11b^+$, $CD45^{int}$) in B6 and CBA mice, as indicated, are shown with corresponding percentages of total leukocytes (B). Data are from one representative experiment of two performed. Statistically significant differences of $P < 0.05$ (*), $P < 0.01$ (**), and $P < 0.001$ (***) are shown.

($P < 0.001$) upregulated in brain tissue taken from both strains of mice with ECM, compared to the naïve control brain tissue, and this upregulation was significantly ($P < 0.001$) greater in the CBA mice (Fig. 2). TNFR2 mRNA expression was also upregulated in both strains during ECM ($P < 0.001$), but there was no difference between strains. Similarly, there were increased levels of LTβ ($P < 0.001$) in ECM brain tissue taken from both strains of mice, although the total levels did not differ between the strains of mice (Fig. 2). Notably, although LTα expression in B6 mouse brains during ECM only reached

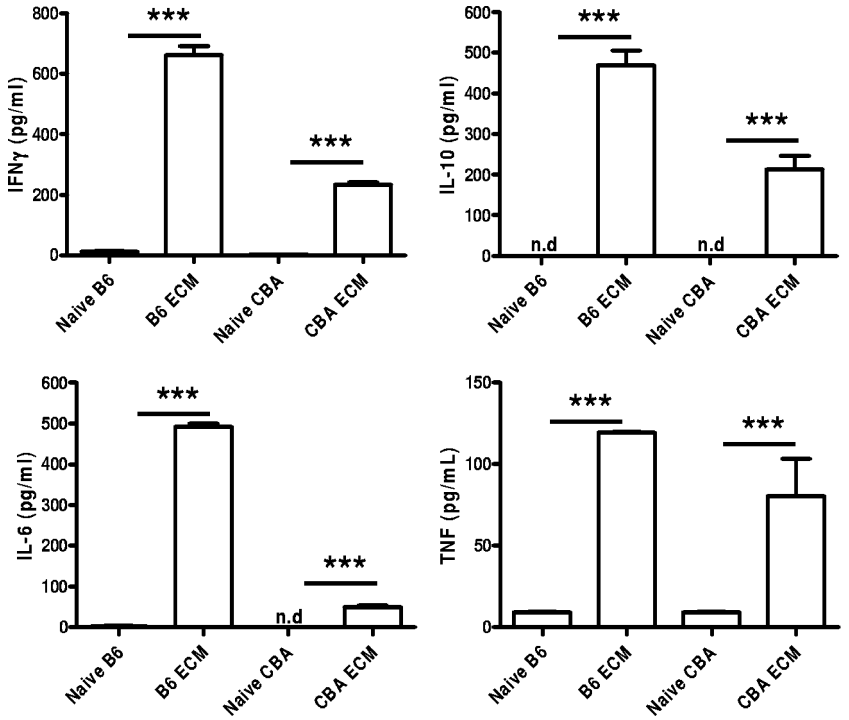

FIG. 4. Levels of serum cytokines differ between CBA and B6 mice during infection. Serum cytokine levels were measured in naïve CBA and B6 mice and *P. berghei* ANKA-infected mice during ECM (mean ± standard error of the mean; $n = 3$ to 5 mice per group), as indicated. Data shown are from one representative experiment of two performed. Statistically significant differences of $P < 0.001$ (***) are shown. IL-10 levels were below the level of detection in naïve mice (n.d, not detected). IL-6 levels were below the level of detection in naïve CBA mice.

the levels of constitutive gene expression observed in naïve CBA brain tissue, the relative change in expression was greater than that observed for CBA mice (Fig. 2). Together, these data further suggest that CBA mice had greater overall immunological activity in the brain during ECM than B6 mice but that there were different patterns of TNF and LTα expression in these two mouse strains.

CBA and B6 mice with ECM have different patterns of cellular recruitment to the brain. We were interested in whether these differences in the brain gene expression profiles of B6 and CBA mice with ECM were also reflected in the leukocyte populations recruited to this site. We analyzed the leukocyte populations in the brains of B6 and CBA mice by FACS when control mice developed ECM (Fig. 3). The recruitment of leukocytes such as T cells (5, 33), NK cells (20), monocytes (40), and neutrophils (43) to the brain following *P. berghei* ANKA infection, as well as the activation of resident microglia (28), is a feature of ECM. Increased numbers of $CD8^+$ T cells, DC, monocytes/macrophages, and neutrophils were found in the brains of both B6 and CBA mice with ECM, compared to naïve controls (Fig. 3). Interestingly, $CD4^+$ T-cell numbers were only found to increase significantly ($P < 0.05$) in B6 mice with ECM, although naïve CBA mice had consistently higher numbers of these cells in their brains. When the numbers of microglia were analyzed, based on the expression of high levels of CD11b and intermediate expression of CD45 (17, 42), numbers were increased in B6 mice with ECM but not CBA mice with ECM (Fig. 3). These data identify relatively minor differences in brain leukocyte composition between B6 and CBA mice with ECM, but nevertheless, these changes may contribute to some of the observed heterogeneity in cerebral gene expression profiles between B6 and CBA mice (Fig. 1).

CBA and B6 mice have different patterns of serum cytokine levels following *P. berghei* ANKA infection. Several differences were also observed between CBA and B6 mice when serum cytokine levels were assessed (Fig. 4). B6 mice had significantly ($P < 0.05$) higher levels of serum IFN-γ, IL-10, and IL-6 than CBA mice with ECM. Thus, despite B6 mice having reduced overall immunological activity in the brain during ECM compared with CBA mice, they generated greater levels of systemic cytokines during infection.

Common strategies to prevent or treat ECM development in B6 and CBA mice. Given the heterogeneity between B6 and CBA mice with ECM and the reported heterogeneity in human CM patients, it was important to determine whether the development of this disease could be prevented in both mouse strains. We (3) and others (48) have recently demonstrated that treatment of C57BL/6 mice with anti-CD25 MAb prior to *P. berghei* ANKA infection protects from ECM. This treatment results in profound changes in the host immune response to *P. berghei* ANKA infection by depleting Treg cells and enhancing parasite-specific $CD4^+$ T-cell activation, events associated with dramatic reductions in parasite burdens (3). Therefore, we next tested if this immunomodulatory treatment prior to *P. berghei* ANKA infection would alter the disease outcome in both ECM-susceptible mouse strains. Following anti-CD25 MAb treatment either on the day prior to infection (data not shown) or 14 days before infection (Fig. 5A), both B6 and CBA

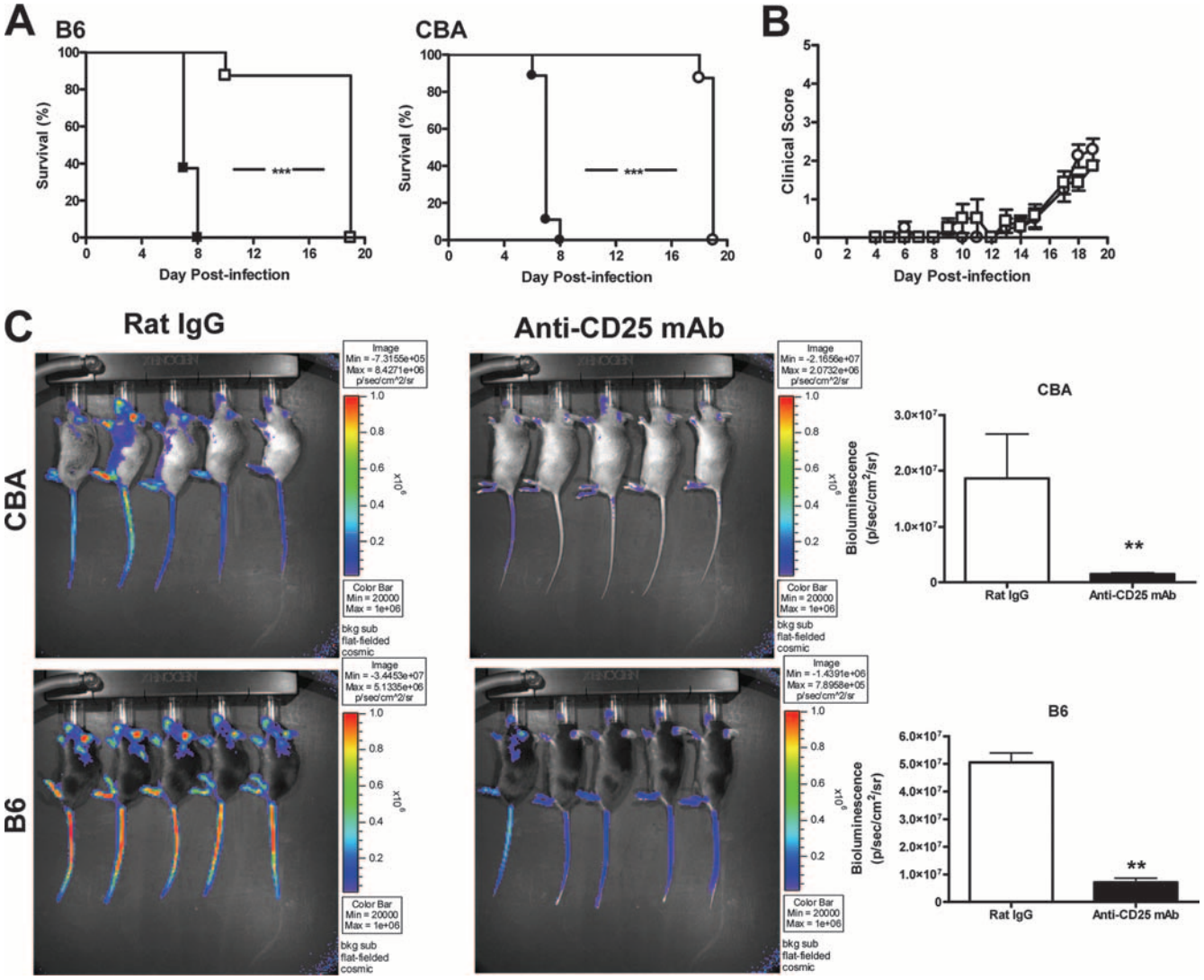

FIG. 5. Depletion of Treg cells prior to infection protects both B6 and CBA mice from ECM. Mice were administered the Treg-depleting anti-CD25 antibody (open symbols) or control rat IgG (closed symbols) 14 days prior to infection and monitored for ECM. B6 (squares; $n = 8$) and CBA mice (circles; $n = 8$) depleted of Treg cells (open symbols) did not develop ECM and survived longer than mice administered control rat IgG (closed symbols) (A). Clinical scores were similar between CBA (open circles) and B6 mice (open squares) depleted of Treg cells (B; mean ± standard error of the mean). Parasite burdens were compared between rat IgG- and anti-CD25 MAb-treated B6 and CBA mice by bioluminescence (C). Mice were administered control rat IgG or anti-CD25 MAb 14 days prior to infection with luciferase-expressing *P. berghei* ANKA. When control mice developed ECM, when clinical scores were ≥3, all groups were anesthetized and injected with luciferin firefly potassium salt and the whole-body parasite burden was visualized with an I-CCD photon-counting video camera and in vivo imaging system. Differences in parasite burdens between control and Treg-depleted mice are depicted in bar graphs as a measurement of bioluminescence. Data shown are from one representative experiment of two performed. Statistically significant differences of $P < 0.01$ (**) and $P < 0.001$ (***) are shown.

mice were protected from ECM, showed few signs of disease, and were culled in the third week of infection with hyperparasitemia and severe anemia according to ethical guidelines (Fig. 5B). All control animals developed ECM (Fig. 5A). Parasite burdens were determined on day 7 p.i. by measuring bioluminescence in mice infected with a transgenic *P. berghei* ANKA line that constitutively expressed luciferase. When ECM symptoms were present in control mice, parasites were observed in the extremities such as the tail, ears, nose, and footpads, where blood vessels were close to the surface of the skin, as well as in tissues such as the lungs and brain (Fig. 5C). Importantly, a significant reduction in the parasite burden ($P < 0.01$) was observed in both B6 and CBA mice treated with anti-CD25 MAb, compared with controls (Fig. 5C), indicating that parasite accumulation in tissue and vasculature was greatly reduced in both mouse strains following anti-CD25 MAb treatment, relative to control animals.

$CD8^+$ T cells also play a key role in the pathogenesis of ECM in C57BL/6 mice, and depletion of this cell population following the onset of ECM symptoms can rescue mice from death (5, 33). To test if this therapy might be more broadly applicable, both B6 and CBA mice were depleted of $CD8^+$ T cells with an anti-CD8 MAb when ECM symptoms were apparent in both mouse strains (day 6 p.i.). Strikingly, this treat-

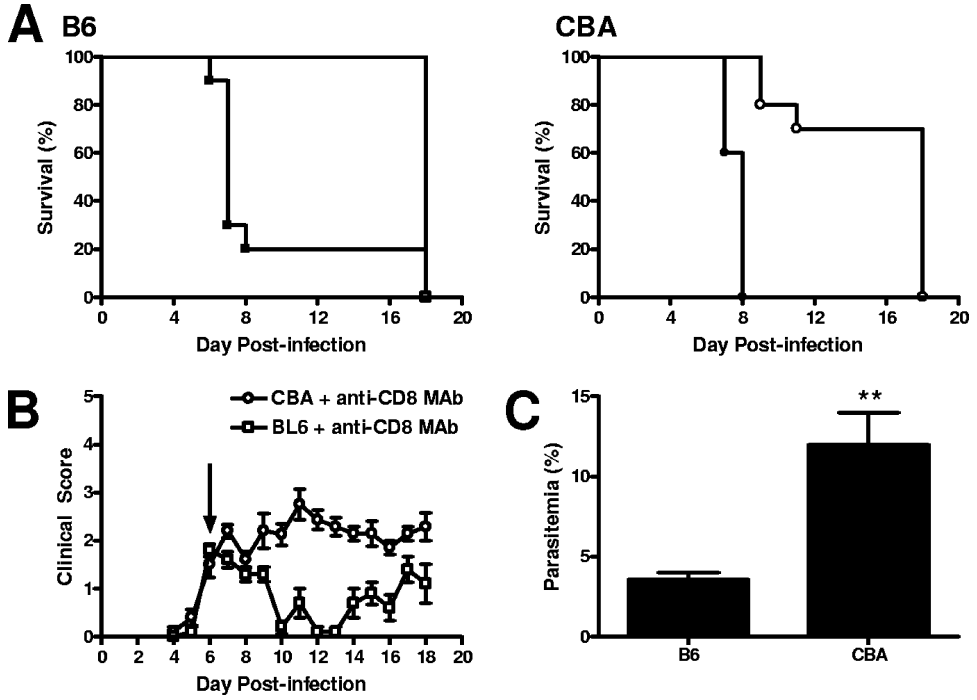

FIG. 6. $CD8^+$ T cells are critical for ECM in B6 and CBA mice, and depletion of these cells halts ECM progression. Anti-CD8 MAb (open symbols) or control rat IgG (closed symbol) was administered i.p. to *P. berghei* ANKA-infected B6 (squares) and CBA (circles) mice on day 6 p.i., when clinical scores were ≥2, and mice were monitored for further disease development (A). B6 (open squares) and CBA (open circles) mice had similar clinical scores upon the administration of anti-CD8 MAb (B; arrow), and these mice were monitored until the development of severe anemia (B). Parasitemia was monitored in anti-CD8 MAb-treated B6 and CBA mice. At 72 h postadministration of the anti-CD8 MAb, differences in parasitemia between the two ECM-susceptible mouse strains were observed (C). Ten mice were included in each group. Statistically significant differences of $P < 0.001$ (***) and $P < 0.002$ (**) are shown.

ment prevented the further development of ECM in B6 and CBA mice (Fig. 6A and B). Interestingly, B6 mice displayed a temporary improvement in clinical scores following this treatment, but this was not the case in CBA mice, whose clinical scores stabilized (Fig. 6A and B). Furthermore, at 72 h following anti-CD8 MAb treatment, blood parasitemia was significantly reduced in B6 mice, but not in CBA mice. The reason for this different effect on blood parasitemia is unknown. Nevertheless, these results indicate that depletion of $CD8^+$ T cells can interrupt the development of ECM in B6 and CBA mice. Anti-CD8 MAb treatment can temporarily reverse or stabilize the progression of ECM in B6 and CBA mice, respectively, with both strains of mice developing hyperparasitemia and severe anemia in the third week of infection. Overall, these prevention and intervention strategies can modulate the outcome of *P. berghei* ANKA infection in B6 and CBA mice, suggesting that, despite clear differences in cellular activity and transcript expression in the brain and in systemic cytokine levels, common immunomodulatory strategies can be used to prevent or treat ECM in both strains of mice.

DISCUSSION

In this study, we found heterogeneous gene expression in brain tissue from B6 and CBA mice with ECM. Many genes associated with ECM in previous microarray studies (13, 44) were also found to be differentially expressed in response to *P. berghei* ANKA in the present analysis. In addition, many specific molecules that have been implicated in ECM pathogenesis were also identified (see Tables S1, S2, and S3 in the supplemental material). A number of genes identified in the present study have yet to be characterized functionally. Therefore, the full impact of the gene expression profiles associated with ECM, and how they might relate to ECM pathogenesis in B6 and CBA mice, remains to be fully appreciated. Also, because the gene expression profiling in this study was performed only once with pooled samples, it is possible that the results communicated here include some false-positive and false-negative results.

B6 and CBA mice both had increased levels of mRNAs encoding TNF, LTα, and their receptors in brain tissue at the onset of ECM. However, changes in TNF and LTα mRNA levels differed between the two mouse strains following *P. berghei* ANKA infection. These trends are in accordance with a study of *P. berghei* ANKA-infected CBA brain tissue taken at day 6 p.i., where increased expression of TNF and LTα mRNAs was also observed (39). Overall, the relative increase in TNF mRNA expression in the brains of CBA mice with ECM was greater than in B6 mice whereas the relative increase in LTα mRNA expression was greater in B6 mice following the onset of ECM. These findings were not unexpected, given the proposed roles for TNF in ECM in CBA mice (18) and LTα in ECM in B6 mice (16).

In addition, some differences in brain leukocyte populations were found when B6 and CBA mice developed ECM, as well

as major differences in serum cytokine levels throughout *P. berghei* ANKA infection. These data suggest that there may be distinct immunological mechanisms involved in ECM pathogenesis in B6 and CBA mice. However, we showed that manipulation of the host immune response to *P. berghei* ANKA infection by depletion of Treg cells or $CD8^+$ T cells resulted in the protection of both B6 and CBA mice from ECM. Of interest, following depletion of $CD8^+$ T cells, B6 mice recovered rapidly, albeit transiently, while CBA mice continued to display clinical signs of *P. berghei* ANKA infection. This observation suggests that physical recovery following $CD8^+$ T-cell depletion depends on different factors in the two strains. Blood parasitemia was transiently reduced in B6 mice receiving anti-CD8 MAb, and this may contribute to their temporary reversal of clinical scores (Fig. 6). This transient reduction in blood parasitemia in B6 mice could be due to several reasons. First, $CD8^+$ cell depletion may cause the parasites to be sequestered to tissue sites and therefore be absent from blood. Second, there may be a population of $CD8^+$ cells that suppresses antiparasitic responses. The removal of all $CD8^+$ cells may remove these suppressor cells, thereby allowing effective immune responses to be generated against the parasite. Third, we cannot discount the possibility that new $CD8^+$ T cells or $CD8^+$ DCs are generated and that these new cells are capable of transient control of parasite growth. The above possibilities are not mutually exclusive and may impact on each other to affect the response of B6 mice to *P. berghei* ANKA infection. Nevertheless, these effects appear to have been different in CBA mice, whose clinical scores stabilize, rather than improve, as is the case with B6 mice.

Parasites sequestered in tissue are thought to be critical for disease pathogenesis during malaria infection (8, 15). Therefore, it is likely that the reduced parasite burdens observed in B6 and CBA mice that received anti-CD25 MAb is a simple explanation for why these animals do not develop ECM. However, we cannot exclude the possibility that this treatment has also altered a critical pathogenic component of the host immune response following *P. berghei* ANKA infection, as this treatment does significantly change antiparasitic immunity (3, 48). Furthermore, our previous data indicate that many of the effects caused by anti-CD25 MAb treatment result from the depletion of Treg cells (3). Others have interpreted the results of this treatment differently and, in particular, have attributed many of the effects of the treatment to the depletion of activated T cells (48). However, we have observed increased $CD4^+$ T-cell activation in mice that have received anti-CD25 MAb, rather than reduced responses (3). Other differences due to the use of this antibody are in the effectiveness of depletion and the duration of this effect, whereby there have been reports of incomplete elimination of $CD25^+$ *FoxP3*$^+$ $CD4^+$ T cells (12). In our experiments, the anti-CD25 MAb treatment resulted in 85 to 95% depletion of $CD25^+$ *FoxP3*$^+$ $CD4^+$ T cells and these cells were reduced in number for at least 14 days, although they did reemerge relatively rapidly following *P. berghei* ANKA infection (3). The reason for the different effects of anti-CD25 MAb treatment may reflect differences in antibody preparation and administration or the immune status of the experimental animals used.

Identifying key molecules involved in CM pathogenesis is vital for the development of treatments to delay or prevent this disease. Information generated from comparisons between ECM-susceptible mouse strains, such as the genes commonly upregulated, may prove important for identifying universal factors that are critical for CM development. These could then be used as potential targets for therapies aimed at preventing or treating CM in humans. Our data suggest that common strategies to delay or prevent CM may be feasible, despite great heterogeneity between individuals in their immune responses during malaria infection.

ACKNOWLEDGMENTS

We thank Paula Hall and Grace Chojnowski for assistance with flow cytometry. We also thank Michelle Gatton for advice on statistical analysis of data.

This work was supported by grants from the Australian NHMRC. L.M.R. is an Australian Postgraduate Award recipient, C.R.E. is an Australian NHMRC Career Development Fellow, and G.R.H. is an Australian NHMRC Practitioner Fellow.

REFERENCES

1. **Adams, S., H. Brown, and G. Turner.** 2002. Breaking down the blood-brain barrier: signaling a path to cerebral malaria? Trends Parasitol. **18:**360–366.
2. **Amani, V., A. M. Vigario, E. Belnoue, M. Marussig, L. Fonseca, D. Mazier, and L. Renia.** 2000. Involvement of IFN-γ receptor-medicated signaling in pathology and anti-malarial immunity induced by Plasmodium berghei infection. Eur. J. Immunol. **30:**1646–1655.
3. **Amante, F. H., A. C. Stanley, L. M. Randall, Y. Zhou, A. Haque, K. McSweeney, A. P. Waters, C. J. Janse, M. F. Good, G. R. Hill, and C. R. Engwerda.** 2007. A role for natural regulatory T cells in the pathogenesis of experimental cerebral malaria. Am. J. Pathol. **171:**548–559.
4. **Bagot, S., M. Idrissa Boubou, S. Campino, C. Behrschmidt, O. Gorgette, J. L. Guenet, C. Penha-Goncalves, D. Mazier, S. Pied, and P. A. Cazenave.** 2002. Susceptibility to experimental cerebral malaria induced by *Plasmodium berghei* ANKA in inbred mouse strains recently derived from wild stock. Infect. Immun. **70:**2049–2056.
5. **Belnoue, E., M. Kayibanda, A. M. Vigario, J. C. Deschemin, N. van Rooijen, M. Viguier, G. Snounou, and L. Renia.** 2002. On the pathogenic role of brain-sequestered αβ $CD8^+$ T cells in experimental cerebral malaria. J. Immunol. **169:**6369–6375.
6. **Boubou, M. I., A. Collette, D. Voegtle, D. Mazier, P. A. Cazenave, and S. Pied.** 1999. T cell response in malaria pathogenesis: selective increase in T cells carrying the TCR Vβ8 during experimental cerebral malaria. Int. Immunol. **11:**1553–1562.
7. **Brown, H., G. Turner, S. Rogerson, M. Tembo, J. Mwenechanya, M. Molyneux, and T. Taylor.** 1999. Cytokine expression in the brain in human cerebral malaria. J. Infect. Dis. **180:**1742–1746.
8. **Burgner, D., W. Xu, K. Rockett, M. Gravenor, I. G. Charles, A. V. Hill, and D. Kwiatkowski.** 1998. Inducible nitric oxide synthase polymorphism and fatal cerebral malaria. Lancet **352:**1193–1194.
9. **Carter, J. A., V. Mung'ala-Odera, B. G. Neville, G. Murira, N. Mturi, C. Musumba, and C. R. Newton.** 2005. Persistent neurocognitive impairments associated with severe falciparum malaria in Kenyan children. J. Neurol. Neurosurg. Psychiatry **76:**476–481.
10. **Clark, I. A.** 1987. Monokines and lymphokines in malarial pathology. Ann. Trop. Med. Parasitol. **81:**577–585.
11. **Clark, I. A., M. M. Awburn, R. O. Whitten, C. G. Harper, N. G. Liomba, M. E. Molyneux, and T. E. Taylor.** 2003. Tissue distribution of migration inhibitory factor and inducible nitric oxide synthase in falciparum malaria and sepsis in African children. Malaria J. **2:**6.
12. **Couper, K. N., D. G. Blount, J. B. de Souza, I. Suffia, Y. Belkaid, and E. M. Riley.** 2007. Incomplete depletion and rapid regeneration of $Foxp3^+$ regulatory T cells following anti-CD25 treatment in malaria-infected mice. J. Immunol. **178:**4136–4146.
13. **Delahaye, N. F., N. Coltel, D. Puthier, L. Flori, R. Houlgatte, F. A. Iraqi, C. Nguyen, G. E. Grau, and P. Rihet.** 2006. Gene-expression profiling discriminates between cerebral malaria (CM)-susceptible mice and CM-resistant mice. J. Infect. Dis. **193:**312–321.
14. **deWalick, S., F. H. Amante, K. A. McSweeney, L. M. Randall, A. C. Stanley, A. Haque, R. D. Kuns, K. P. MacDonald, G. R. Hill, and C. R. Engwerda.** 2007. Cutting edge: conventional dendritic cells are the critical APC required for the induction of experimental cerebral malaria. J. Immunol. **178:**6033–6037.
15. **Dondorp, A. M., V. Desakorn, W. Pongtavornpinyo, D. Sahassananda, K. Silamut, K. Chotivanich, P. N. Newton, P. Pitisuttithum, A. M. Smithyman, N. J. White, and N. P. Day.** 2005. Estimation of the total parasite biomass in acute falciparum malaria from plasma PfHRP2. PLoS Med. **2:**e204.

16. **Engwerda, C. R., T. L. Mynott, S. Sawhney, J. B. De Souza, Q. D. Bickle, and P. M. Kaye.** 2002. Locally up-regulated lymphotoxin alpha, not systemic tumor necrosis factor alpha, is the principle mediator of murine cerebral malaria. J. Exp. Med. **195:**1371–1377.
17. **Ford, A. L., A. L. Goodsall, W. F. Hickey, and J. D. Sedgwick.** 1995. Normal adult ramified microglia separated from other central nervous system macrophages by flow cytometric sorting. Phenotypic differences defined and direct ex vivo antigen presentation to myelin basic protein-reactive $CD4^+$ T cells compared. J. Immunol. **154:**4309–4321.
18. **Grau, G. E., L. F. Fajardo, P. F. Piguet, B. Allet, P. H. Lambert, and P. Vassalli.** 1987. Tumor necrosis factor (cachectin) as an essential mediator in murine cerebral malaria. Science **237:**1210–1212.
19. **Grau, G. E., H. Heremans, P. F. Piguet, P. Pointaire, P. H. Lambert, A. Billiau, and P. Vassalli.** 1989. Monoclonal antibody against interferon gamma can prevent experimental cerebral malaria and its associated overproduction of tumor necrosis factor. Proc. Natl. Acad. Sci. USA **86:**5572–5574.
20. **Hansen, D. S., N. J. Bernard, C. Q. Nie, and L. Schofield.** 2007. NK cells stimulate recruitment of $CXCR3^+$ T cells to the brain during Plasmodium berghei-mediated cerebral malaria. J. Immunol. **178:**5779–5788.
21. **Hansen, D. S., M. A. Siomos, L. Buckingham, A. A. Scalzo, and L. Schofield.** 2003. Regulation of murine cerebral malaria pathogenesis by CD1d-restricted NKT cells and the natural killer complex. Immunity **18:**391–402.
22. **Hermsen, C., T. van de Wiel, E. Mommers, R. Sauerwein, and W. Eling.** 1997. Depletion of $CD4^+$ or $CD8^+$ T-cells prevents Plasmodium berghei induced cerebral malaria in end-stage disease. Parasitology **114**(Pt. 1)**:**7–12.
23. **Kern, P., C. J. Hemmer, J. Van Damme, H. J. Gruss, and M. Dietrich.** 1989. Elevated tumor necrosis factor alpha and interleukin-6 serum levels as markers for complicated Plasmodium falciparum malaria. Am. J. Med. **87:**139–143.
24. **Kossodo, S., C. Monso, P. Juillard, T. Velu, M. Goldman, and G. E. Grau.** 1997. Interleukin-10 modulates susceptibility in experimental cerebral malaria. Immunology **91:**536–540.
25. **Kwiatkowski, D., A. V. Hill, I. Sambou, P. Twumasi, J. Castracane, K. R. Manogue, A. Cerami, D. R. Brewster, and B. M. Greenwood.** 1990. TNF concentration in fatal cerebral, non-fatal cerebral, and uncomplicated Plasmodium falciparum malaria. Lancet **336:**1201–1204.
26. **Lou, J., R. Lucas, and G. E. Grau.** 2001. Pathogenesis of cerebral malaria: recent experimental data and possible applications for humans. Clin. Microbiol. Rev. **14:**810–820.
27. **Mackintosh, C. L., J. G. Beeson, and K. Marsh.** 2004. Clinical features and pathogenesis of severe malaria. Trends Parasitol. **20:**597–603.
28. **Medana, I. M., N. H. Hunt, and T. Chan-Ling.** 1997. Early activation of microglia in the pathogenesis of fatal murine cerebral malaria. Glia **19:**91–103.
29. **Miu, J., A. J. Mitchell, M. Muller, S. L. Carter, P. M. Manders, J. A. McQuillan, B. M. Saunders, H. J. Ball, B. Lu, I. L. Campbell, and N. H. Hunt.** 2008. Chemokine gene expression during fatal murine cerebral malaria and protection due to CXCR3 deficiency. J. Immunol. **180:**1217–1230.
30. **Mung'Ala-Odera, V., R. W. Snow, and C. R. Newton.** 2004. The burden of the neurocognitive impairment associated with Plasmodium falciparum malaria in sub-Saharan Africa. Am. J. Trop. Med. Hyg. **71:**64–70.
31. **Murphy, S. C., and J. G. Breman.** 2001. Gaps in the childhood malaria burden in Africa: cerebral malaria, neurological sequelae, anemia, respiratory distress, hypoglycemia, and complications of pregnancy. Am. J. Trop. Med. Hyg. **64:**57–67.
32. **Nagayasu, E., K. Nagakura, M. Akaki, G. Tamiya, S. Makino, Y. Nakano, M. Kimura, and M. Aikawa.** 2002. Association of a determinant on mouse chromosome 18 with experimental severe *Plasmodium berghei* malaria. Infect. Immun. **70:**512–516.
33. **Nitcheu, J., O. Bonduelle, C. Combadiere, M. Tefit, D. Seilhean, D. Mazier, and B. Combadiere.** 2003. Perforin-dependent brain-infiltrating cytotoxic $CD8^+$ T lymphocytes mediate experimental cerebral malaria pathogenesis. J. Immunol. **170:**2221–2228.
34. **Ohno, T., and M. Nishimura.** 2004. Detection of a new cerebral malaria susceptibility locus, using CBA mice. Immunogenetics **56:**675–678.
35. **Oo, M. M., M. Aikawa, T. Than, T. M. Aye, P. T. Myint, I. Igarashi, and W. C. Schoene.** 1987. Human cerebral malaria: a pathological study. J. Neuropathol. Exp. Neurol. **46:**223–231.
36. **Pamplona, A., A. Ferreira, J. Balla, V. Jeney, G. Balla, S. Epiphanio, A. Chora, C. D. Rodrigues, I. P. Gregoire, M. Cunha-Rodrigues, S. Portugal, M. P. Soares, and M. M. Mota.** 2007. Heme oxygenase-1 and carbon monoxide suppress the pathogenesis of experimental cerebral malaria. Nat. Med. **13:**703–710.
37. **Porta, J., A. Carota, G. P. Pizzolato, E. Wildi, M. C. Widmer, C. Margairaz, and G. E. Grau.** 1993. Immunopathological changes in human cerebral malaria. Clin. Neuropathol. **12:**142–146.
38. **Potter, S., T. Chan-Ling, H. J. Ball, H. Mansour, A. Mitchell, L. Maluish, and N. H. Hunt.** 2006. Perforin mediated apoptosis of cerebral microvascular endothelial cells during experimental cerebral malaria. Int. J. Parasitol. **36:**485–496.
39. **Rae, C., J. A. McQuillan, S. B. Parekh, W. A. Bubb, S. Weiser, V. J. Balcar, A. M. Hansen, H. J. Ball, and N. H. Hunt.** 2004. Brain gene expression, metabolism, and bioenergetics: interrelationships in murine models of cerebral and noncerebral malaria. FASEB J. **18:**499–510.
40. **Rest, J. R.** 1982. Cerebral malaria in inbred mice. I. A new model and its pathology. Trans. R. Soc. Trop. Med. Hyg. **76:**410–415.
41. **Schofield, L., M. J. McConville, D. Hansen, A. S. Campbell, B. Fraser-Reid, M. J. Grusby, and S. D. Tachado.** 1999. CD1d-restricted immunoglobulin G formation to GPI-anchored antigens mediated by NKT cells. Science **283:**225–229.
42. **Sedgwick, J. D., S. Schwender, H. Imrich, R. Dorries, G. W. Butcher, and V. ter Meulen.** 1991. Isolation and direct characterization of resident microglial cells from the normal and inflamed central nervous system. Proc. Natl. Acad. Sci. USA **88:**7438–7442.
43. **Senaldi, G., C. Vesin, R. Chang, G. E. Grau, and P. F. Piguet.** 1994. Role of polymorphonuclear neutrophil leukocytes and their integrin CD11a (LFA-1) in the pathogenesis of severe murine malaria. Infect. Immun. **62:**1144–1149.
44. **Sexton, A. C., R. T. Good, D. S. Hansen, M. C. D'Ombrain, L. Buckingham, K. Simpson, and L. Schofield.** 2004. Transcriptional profiling reveals suppressed erythropoiesis, up-regulated glycolysis, and interferon-associated responses in murine malaria. J. Infect. Dis. **189:**1245–1256.
45. **Snow, R. W., M. H. Craig, C. R. Newton, and R. W. Steketee.** 2003. The public health burden of Plasmodium falciparum malaria in Africa: deriving the numbers. Disease Control Priorities Project working paper no. 11. Fogarty International Center, National Institutes of Health, Bethesda, MD.
46. **Sun, G., W. L. Chang, J. Li, S. M. Berney, D. Kimpel, and H. C. van der Heyde.** 2003. Inhibition of platelet adherence to brain microvasculature protects against severe *Plasmodium berghei* malaria. Infect. Immun. **71:**6553–6561.
47. **van der Heyde, H. C., I. Gramaglia, G. Sun, and C. Woods.** 2005. Platelet depletion by anti-CD41 (αIIb) mAb injection early but not late in the course of disease protects against Plasmodium berghei pathogenesis by altering the levels of pathogenic cytokines. Blood **105:**1956–1963.
48. **Vigário, A. M., O. Gorgette, H. C. Dujardin, T. Cruz, P. A. Cazenave, A. Six, A. Bandeira, and S. Pied.** 2007. Regulatory $CD4^+$ $CD25^+$ $Foxp3^+$ T cells expand during experimental Plasmodium infection but do not prevent cerebral malaria. Int. J. Parasitol. **37:**963–973.
49. **Yañez, D. M., D. D. Manning, A. J. Cooley, W. P. Weidanz, and H. C. van der Heyde.** 1996. Participation of lymphocyte subpopulations in the pathogenesis of experimental murine cerebral malaria. J. Immunol. **157:**1620–1624.
50. **Yeo, T. W., D. A. Lampah, R. Gitawati, E. Tjitra, E. Kenangalem, Y. R. McNeil, C. J. Darcy, D. L. Granger, J. B. Weinberg, B. K. Lopansri, R. N. Price, S. B. Duffull, D. S. Celermajer, and N. M. Anstey.** 2007. Impaired nitric oxide bioavailability and L-arginine reversible endothelial dysfunction in adults with falciparum malaria. J. Exp. Med. **204:**2693–2704.

Editor: J. F. Urban, Jr.